PHYSICAL REVIEW B VOLUME 18, NUMBER 8 15 OCTOBER 1978

Elastic constants in Nb-Zr alloys from zero temperature to the melting point: Experiment and theory

J. Ashkenazi, M. Dacorogna, M. Peter, Y. Talmor, and E. Walker
Département de Physique de la Matière Condensée, Université de Genève, Suisse

S. Steinemann
Institut de Physique Expérimentale, Université de Lausanne, Suisse

(Received 11 January 1978)

The elastic constants of bcc Nb-Zr alloys are measured over a composition range between 100 and 30 at.% of Nb and temperatures between zero and the melting point, using a new technique for the high-temperature measurements. Anomalous behavior is found for C_{44}. The anomaly is a band-structure effect which is corroborated by theoretical calculations using electron-lattice coupling constants derived from a tight-binding parametrization scheme. The calculation is of a type similar to phonon dispersion ones, having the further complication of temperature effects which have convergence difficulties and need a special interpolation method.

I. INTRODUCTION

An anomalous behavior of the trigonal shear constant C_{44} versus temperature has been observed in $3d$, $4d$, and $5d$ transition metals of the tenth column with fcc structure and of the fifth column with bcc structure. This is the case for Pd, Pt, Nb, and also for V and Ta as was measured recently by one of us (E. W.). The band structures of these metals have the common feature that the Fermi level lies 10–20 mRy from the top of a density-of-states peak, and that the Fermi surfaces contain open and closed sheets[1-5] (case of Nb: Fig. 1). This common feature seems to be the reason for a similar type of anomaly in all of them, and Nb is the one which exhibits the largest anomaly.

Since elastic constants are related to acoustic phonons in the zero-momentum limit, an anomaly in C_{44} is probably followed by one in the appropriate low-momentum transversal phonon. Such an anomaly exists in the phonon spectrum of Nb,[6,7] and might have an effect on its superconducting properties. So a detailed experimental and theoretical study of the C_{44} anomaly in Nb is associated with the attempt to understand phonon anomalies and superconductivity in this substance, which is becoming a subject of wide interest.[8,9]

The underlying idea of this work is to study the elastic constants in Nb as a function of two parameters, temperature and number of electrons per atom. Temperature effects are measured from close to zero up to the melting point, and the variation in the number of electrons is achieved by alloying.

A suitable element to alloy with Nb for such measurements seems to be Zr. It has one electron less per atom, and the alloy's bcc phase is stable over a wide range of composition. Moreover, as far as the relation with superconductivity is of interest, the maximal T_c in the substance is for 25-at.% Zr.[10] As for previous elastic constant measurements, the only available data are those of Armstrong *et al.*[11] on a pure Nb single crystal, of Hayes and Brotzen[12] on few Nb-rich Nb-Zr single crystals, and of Goasdoue *et al.*[13] on Zr-rich single crystals. No systematic measurements have been done in the past over a wide range of compositions and at temperatures close to the melting point.

For such a task two major technical difficulties have to be overcome, namely, the growth of Nb-Zr single crystals over a wide composition range and the performance of ultrasonic measurements at very high temperatures. In previous publications,[14,15] low-temperature measurements of Nb-Zr single crystals up to 70-at.% Zr and high-temperature measurements for pure Nb have been presented. Here we present results for the same samples as in Ref. 14 at the whole temperature range up to the melting point.

The anomalous behavior obtained for the elastic constants is explained by a calculation based on the band structure of Nb, and the electron-lattice coupling constants. The basic idea and formulas have been presented in a previous work.[16] The method is equivalent to a tight-binding calculation of the electronic contribution to the zero-momentum-limit phonon spectrum, using electron-phonon coupling constants based on a moving-wave-functions basis.

The rigorous formulation of the electron-phonon coupling problem in terms of a moving basis, and its relation with the Bloch formulation, is

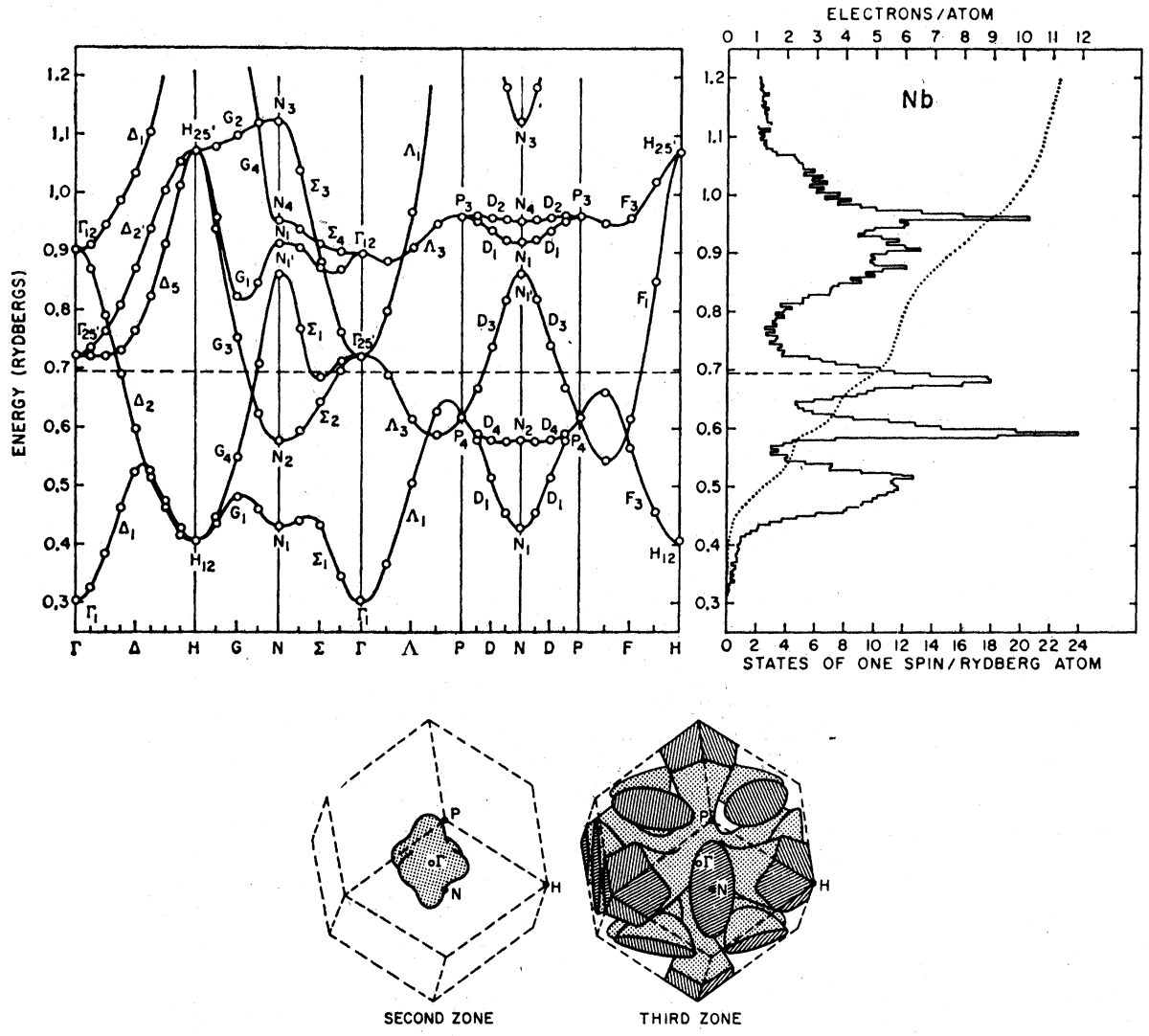

FIG. 1. Results of Mattheiss (Ref. 1) for the band structure, the density of states and the Fermi surface of Nb.

presented elsewhere.[17] In our opinion such a method provides fast convergence for electron-phonon coupling calculations in transition metals. The same electron-phonon parameters used here have been used in a previous work[18] solving unrestrictedly the Eliashberg equations for Nb, obtaining the anisotropic mass renormalization and superconducting gap function. The calculated mass renormalization anisotropy is found to agree with recent de Haas–van Alphen (dHvA) results.[19] The moving-wave-function basis for the electron-phonon coupling has been used recently also be Varma *et al.*[9]

A partial description of the theoretical part of this work is presented in Ref. 20.

II. EXPERIMENTAL PROCEDURE

A. Method

The detailed description of the Nb-Zr single crystals growth is given in Ref. 14. To determine the sound velocities, we use the classical pulse echo technique. In the low-temperature region (4.2–300 K) the transducer was bound directly to the crystal by means of Nonaq stopcock lubricant under 200 K and salool between 200 and 300 K. Above room temperature we use a technique which is equivalent, in principle, to that described by Lowrie and Gonas[21] but with slight modifications. The experimental setup for ultrasonic measurements is shown in Fig. 2. It is essentially the

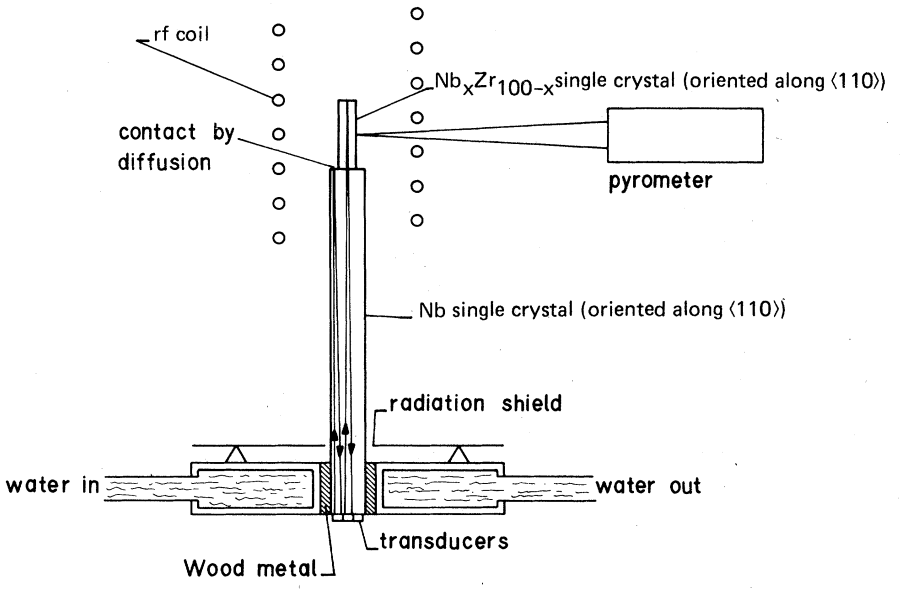

FIG. 2. Experimental setup for the high-temperature ultrasonic measurements (details are given in the text).

same as that described previously for a pure Nb single crystal.[15] Using this method one measures the time delay between two echoes of an ultrasonic wave reflected from two parallel surfaces of the sample where only the sample's portion between those two surfaces is homogeneously heated.

Large single crystals of pure Nb were available and it was thus possible to make a step cut on them and produce the two required parallel surfaces. This could not be done for the Nb-Zr alloys. Those single crystals have been grown quite small, of 15–20 mm in length and about 5 mm in diameter, which excludes making any step cut on them. This difficulty is overcome by welding the small Nb-Zr single crystal on the top of a sufficiently large pure Nb single crystal. The welding is done by diffusion at about 1500°C. If pressure is applied on the contact surfaces, then the time needed for such an operation does not exceed 1 h. Otherwise it takes several days. After completing the measurement, the sample is separated from its pedestal (wave guide or buffer rod) by spark cutting and the base is usable for another experiment. All the measurements are done with the same Nb wave guide of 10 cm length and 10 mm diameter.

The Nb-Zr single crystals as well as the pure Nb wave guide are oriented in the [110] direction. This allows the determination of the three independent elastic constants (see Sec. II) by measuring the sound velocity of the pure longitudinal mode v_l and the two pure nondegenerate transverse modes v_{t1} and v_{t2}. They are related to the elastic constants by the well-known relations

$$\rho v_l^2 = \tfrac{1}{2}(C_{11} + C_{12} + 2C_{44}) \tag{1a}$$

for the longitudinal mode,

$$\rho v_{t1}^2 = C_{44} \tag{1b}$$

for the C transverse mode, and

$$\rho v_{t2}^2 = \tfrac{1}{2}(C_{11} - C_{12}) \tag{1c}$$

for the C' transverse mode.

In order to excite a pure elastic transverse mode in the sample in its maximum intensity, one must use the pure transverse mode in the wave guide which is the least attenuated. In pure Nb and also in the Nb-Zr alloys, the C' mode is much more attenuated than the C mode. This fact was attributed by P. A. Maeusli and S. Steinemann (private communication) to the relaxation of interstitial oxygen atoms during the C' mode deformation. For this reason we use the C transverse mode in the Nb wave guide to excite both C and C' modes in the samples. This means that the wave guide and the sample are oriented such as their [001] directions are parallel for the C mode and perpendicular for the C' mode. Therefore, two diffusions have to be made for measuring the transverse modes. Attenuation is small for the longitudinal mode, on the other hand.

The sample is heated using an rf coil keeping the transducer contacting Nb face at room temperature by water cooling. The large temperature gradient affects mainly the traveling wave in the Nb portion and not the measurements. Nevertheless, a small temperature gradient remains in the sample. It can be reduced to a minimum by an optimal choice of the sample position inside the rf coil, but cannot be totally eliminated. In our case, the maximal temperature difference along

the sample has been kept below 50°C in the whole temperature range. Moreover, since the variation of the elastic constants is small and almost linear, the effect of this gradient can be reduced by considering the average temperature. This is possible above 1000°C where a two-color Leybold pyrometer is used for temperature measurements. In the range, between room temperature and 1000°C, we use a chromel-alumel thermocouple dipped in a piece of copper, pressed on the free face of the sample through a thin plate of sapphire, avoiding any diffusion of copper into the crystals. This sapphire plate, which gives a relatively poor thermal contact between the sample and the thermocouple, introduces errors in the measured temperatures. Those errors are reduced by making measurements with increasing and decreasing temperature (it is not possible to achieve stabilization in this range), but there still remains an uncertainty of ±50°C. For temperatures higher than 1000°C stabilization can be achieved and those errors do not exceed 10°C. Below room temperature the method described in Ref. 14 enables temperature accuracy of ±2°C.

All the time measurements between the two first echoes resulting from the 10-MHz pulses are performed on a Tektronix oscilloscope with time delay plug-in unit which displays directly the time difference between any two points on the screen. This technique is not very accurate, but it is difficult to measure small differences in the delay time between two echoes when the overall delay has a much higher inaccuracy due to the variation in the temperature gradient along the Nb wave guide. The displayed time value has a resolution of 0.01 μsec as long as time is less than 15 μsec; otherwise it has only resolution of 0.1 μsec. In our case, the delay between echoes is generally larger than 15 μsec and a one-digit accuracy is lost. Because of this fact, measuring points do not follow a smooth curve.

B. Results

The results measured for the two transverse and the longitudinal elastic constants given in Equations (1a)–(1c) are shown in Figs. 3 and 4. In Fig. 5 we present the bulk modulus $B = \frac{1}{3}(C_{11} + 2C_{12})$ determined mathematically from those results. These results are characterized by the following systematic anomalous behavior.

In the low-temperature range C_{44} has a minimum which shifts down in the temperature scale from 450 K for pure Nb to 60 K for 75-at.% Nb. Decreasing the Nb percentage further, this minimum shifts up in the temperature scale and persists as a change of slope; it disappears for 30-at.%Nb. The 75-at.%Nb composition case is also the one with the maximal superconducting T_c.[10] Using the rigid-band approximation, it is around this composition where the Fermi level crosses the top of the density-of-states peak.[1]

In the high-temperature range, the slopes of the C_{44} curves change rapidly with composition, and they all cross around 900 K. The slopes of C_{44} and of $C' = \frac{1}{2}(C_{11} - C_{12})$ decrease towards the melting points. The temperature at which this slope decrease starts goes down as the Zr percentage increases.

III. THEORETICAL CALCULATION OF ELASTIC CONSTANTS

The theoretical calculation is based on a distance-dependent tight-binding parametrization of the APW result of Mattheiss for Nb (Fig. 1), and a Brillouin zone summation of matrix elements obtained from those parameters, used to evaluate the elastic constants as functions of temperature and composition. The theoretical elastic constants are isothermal and not adiabatic (as measured by experiment). However, the difference between the two is believed to be small compared with the inaccuracies involved in the calculation.

A. Tight-binding parametrization

The effective tight-binding transfer integrals determining the band structure are expressed as functions of distance in terms of several parameters. Such a procedure is useful both to reduce the number of parameters required and to determine the electron-lattice coupling constants. This parametrization is based on the generalization of the method of Ashkenazi and Weger[22] which has been used in parametrizing the band structure of V_3Ga,[23] and also by Birnboim and Gutfreund[24] calculating electron-phonon coupling constants. The method is now described.

The Bloch functions are assumed to be linear combinations of the functions

$$\psi_{lm}(\vec{k}, \vec{r}) = \frac{1}{\sqrt{N}} \sum_{\vec{R}} e^{i\vec{k}\cdot\vec{R}} \phi_{lm}(\vec{r} - \vec{R}) , \tag{2}$$

where

$$\phi_{lm}(\vec{r}) = (1/r) R_l(r) Y_{lm}(\Omega) , \tag{3}$$

$\vec{R}$ are the equilibrium lattice positions, and l are taken as 0 and 2, considering the 4d and 5s bands. The two-center transfer integrals are given by

$$J_{lm}^{l'm'}(\vec{R}) = \int \phi_{lm}(\vec{r}) V(\vec{r}) \phi_{l'm'}(\vec{r} - \vec{R})\, d^3r , \tag{4}$$

where $V(\vec{r})$ is an atomic contribution to the lattice potential, assumed here to be spherically sym-

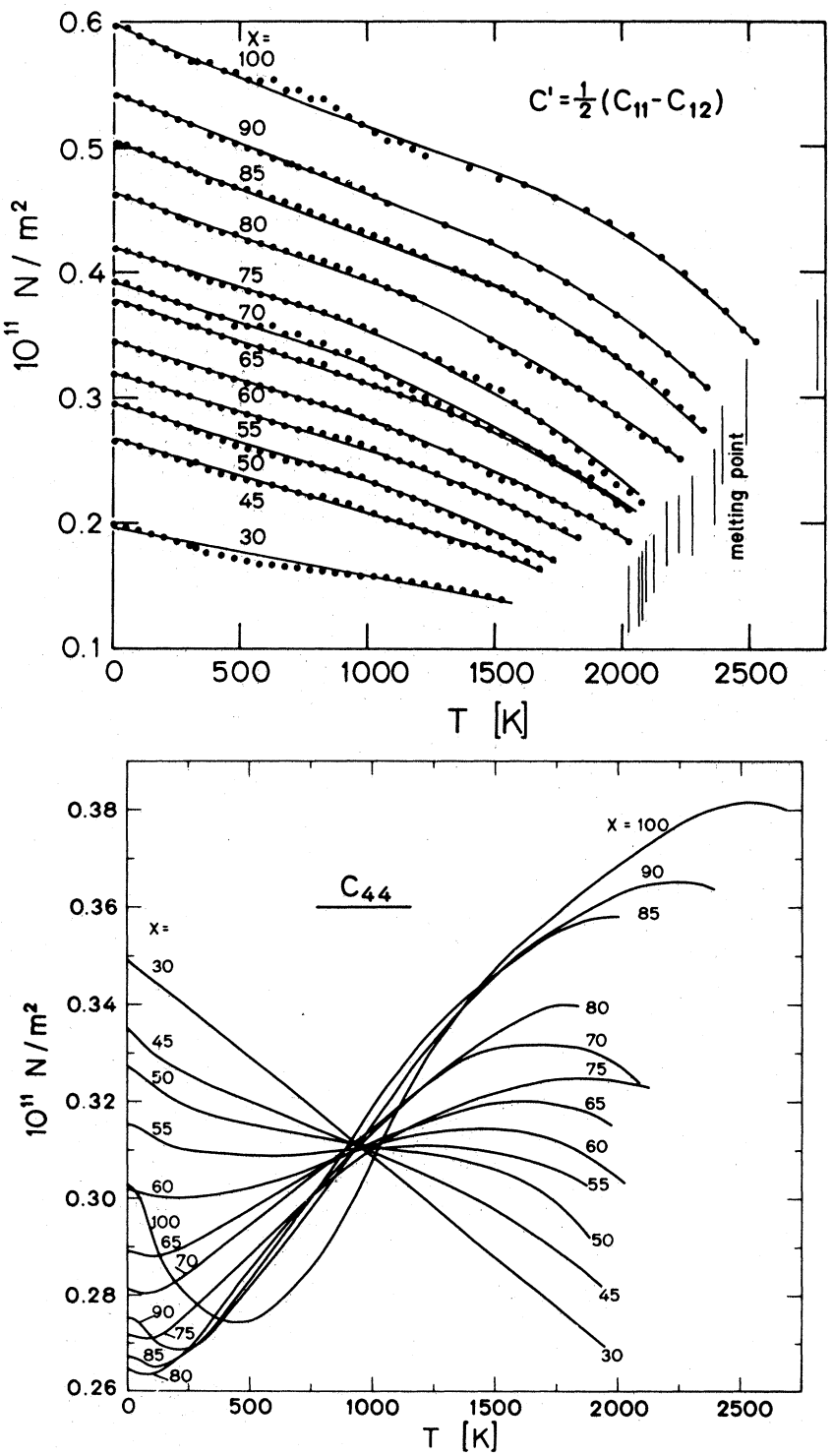

FIG. 3. Experimental results for the two shear moduli in Nb_xZr_{100-x}.

metric. It has been shown in Ref. 22 that for tightly bound electrons, the main contribution to $J^{l'm'}_{lm}(\vec{R})$ in Eq. (4) comes from a region where $\phi_{l'm'}(\vec{r}-\vec{R})$ has its asymptotic behavior.

Let us assume that the asymptotic behavior is given by

$$R_l(r) \underset{r\to\infty}{\longrightarrow} A_l r^{P_l} \exp(-Q_l r)\,, \tag{5}$$

where A_l, P_l, and Q_l ($l=0,2$) are parameters.

Following Ref. 22 we expand the asymptotic form

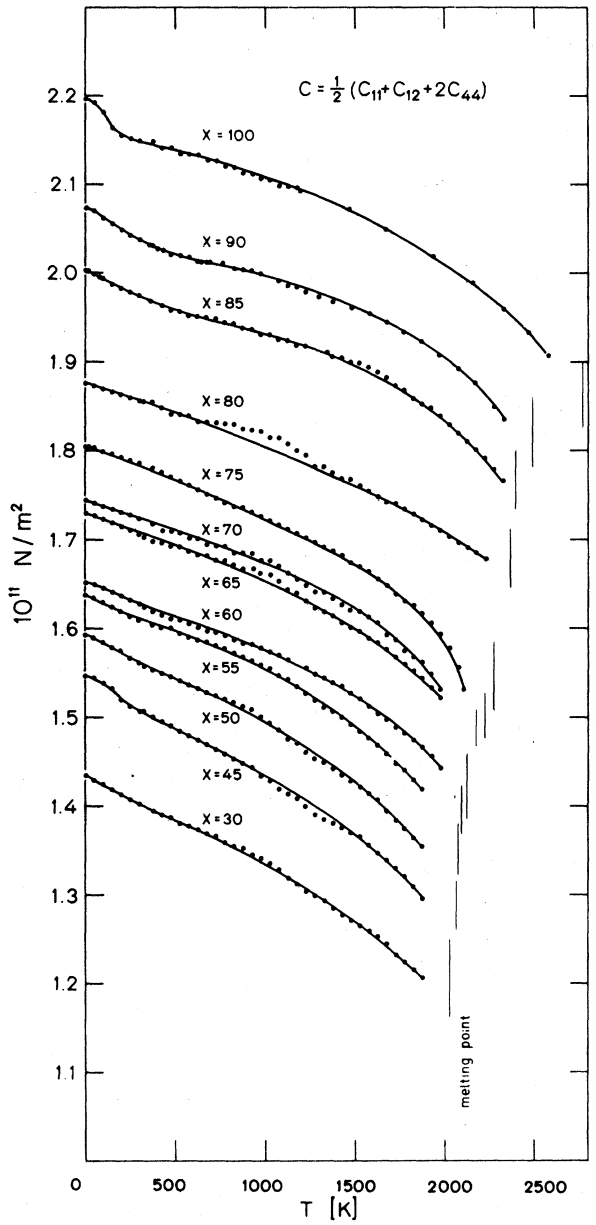

FIG. 4. Experimental results for the "longitudinal" elastic constant in Nb_xZr_{100-x}.

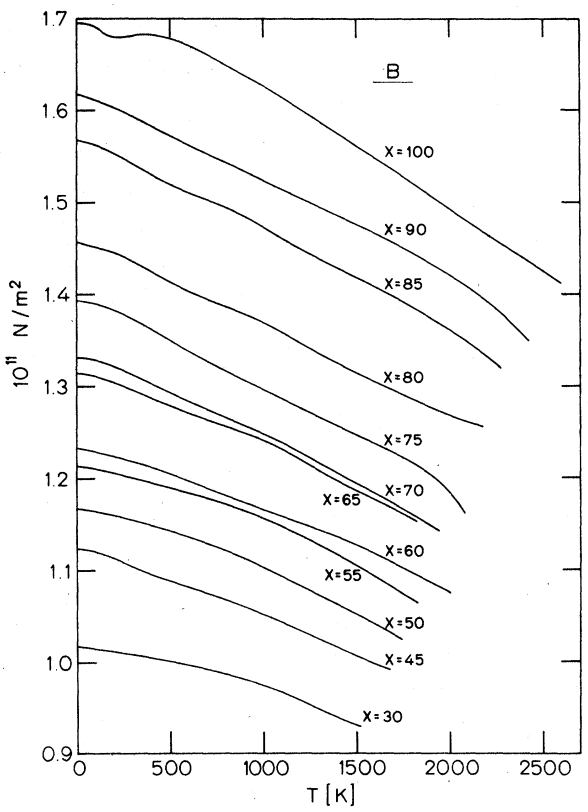

FIG. 5. Results derived from experiment for the bulk modulus $B=\frac{1}{3}(C_{11}+2C_{12})$ in Nb_xZr_{100-x}.

of $\phi_{l'm'}(\vec{r}-\vec{R})$ in power series of r/R. Using spherical coordinates around $\vec{r}=0$, and doing the integration (4) we consider only the leading nonvanishing terms. So doing one gets distance-dependent integrals expressed in terms of the parameters Q_l, P_l, and $B_{ll'}$, the last being a multiplication of A_l, with a radial integral including $R_l(r)$. The resulting expression for the Slater-Koster transfer integrals are given in Table I.

The band structure of Nb (Fig. 1)[1] is fitted by those parameters considering neighbors up to the third shell, and also considering two additional crystal-field-splitting integrals as parameters. The effects of three-center integrals and of overlap integrals between wave functions centered on neighboring atoms are neglected. The values obtained for the band integrals and their distance derivatives are given in Table II. (The distance dependence of the crystal-field-splitting integrals is neglected.) For the d transfer integrals a behavior close to R^{-5} is obtained, which is approximately the one expected from resonance theories.[25]

Using the band parameters given in Table II, and the s-d Slater-Koster angular coefficients given in previous publications[16,26] (in terms of the direction cosines l_i, $i=1,2,3$) a tight-binding 6×6 space Hamiltonian matrix $\underline{H}(\vec{R})$ is constructed. This space Hamiltonian is Fourier transformed and diagonalized giving the band energies (fitted to Mattheiss' results)

$$E_{b\vec{k}}=\sum_{lm}[U^b_{lm}(\vec{k})]^*\left(\sum_{\vec{R}}e^{i\vec{k}\cdot\vec{R}}H^{lm'}_{lm}(\vec{R})\right)U^b_{l'm'}(\vec{k}), \quad (6)$$

where $\underline{U}(\vec{k})$ is the eigenvector unitary matrix transforming the basis functions given in Eq. (2)

TABLE I. Expressions for the two-center transfer integrals as functions of the interatomic distance R, in terms of the parameters $B_{ll'}$, Q_l, and P_l ($l=0,2$).

Integral	
$dd\sigma(R)$	$(B_{22}/R^3)\exp(-Q_2R)[1+\frac{1}{3}(1-P_2)(3-P_2)$ $+\frac{1}{3}(3-2P_2)Q_2R+\frac{1}{3}(Q_2R)^2]$
$dd\pi(R)$	$-(B_{22}/R^3)\exp(-Q_2R)(2-P_2+Q_2R)$
$dd\delta(R)$	$(B_{22}/R^3)\exp(-Q_2R)$
$ss\sigma(R)$	$(B_{00}/R)\exp(-Q_0R)$
$sd\sigma(R)$	$(B_{02}/R)\exp(-Q_2R)+(B_{20}/R^3)\exp(-Q_0R)$ $[\frac{1}{3}(1-P_0)(3-P_0)+\frac{1}{3}(3-2P_0)Q_0R+\frac{1}{3}(Q_0R)^2]$

to the Bloch eigenfunctions, and b is the band index.

B. Derivation of the elastic constants

There have been several errors in the formulas derived in Ref. 16, so they are rederived, making some generalizations.

Assuming a crystal undergoing a deformation given to the first order by

$$\delta R_i=\sum_j \bar{\epsilon}_{ij}R_j \tag{7}$$

the strain tensor $\underline{\epsilon}$ is defined by

$$\epsilon_{ij}=(1-\tfrac{1}{2}\delta_{ij})(\bar{\epsilon}_{ij}+\bar{\epsilon}_{ji}). \tag{8}$$

According to Hooke's law, the bilinear increase in the free energy per unit volume due to the deformation is given by

$$\delta F=\frac{1}{2}\sum_{\alpha\beta} C_{\alpha\beta}\epsilon_\alpha\epsilon_\beta, \tag{9}$$

where, using the Voigt notation, a vector index $\alpha=1,\ldots,6$ is equivalent to a pair of matrix indices $ij=11$, 22, 33, 23, 13, 12, respectively.

The tensor of the elastic constants, $\underline{C}$, is symmetric, and for a cubic system it contains only three different elements C_{11}, C_{12}, and C_{44} represented before Eq. (1) (the other elements being either equal to those or to zero by symmetry).

Diagonalizing the $\underline{C}$ matrix, one gets three different elements:

$$B=\tfrac{1}{3}G_0=\tfrac{1}{3}(C_{11}+2C_{12}) \tag{10a}$$

is the bulk modulus,

TABLE II. Values, in rydbergs, of the crystal-field splitting, the Slater-Koster transfer integrals, and their distance (R) first and second derivatives, used for Nb in this work.

	R	$dd\sigma$	$dd\pi$	$dd\delta$	$ss\sigma$	$sd\sigma$	K_{ds} [a]	K_{et} [b]
	0						−0.064 77	−0.099 57
Integral	$a_0\sqrt{3}/2$	−0.085 70	0.079 09	−0.024 52	−0.072 88	−0.068 92		
$f(R)$	a_0 [c]	−0.048 09	0.041 68	−0.011 83	−0.049 59	−0.050 64		
	$a_0\sqrt{2}$	−0.010 35	0.007 41	−0.001 67	−0.016 64	−0.018 18		
First derivative	$a_0\sqrt{3}/2$	−3.922	−4.325	−4.921	−2.559	−1.879		
	a_0	−4.118	−4.588	−5.218	−2.800	−2.394		
$\frac{R}{f}\frac{df}{dR}$	$a_0\sqrt{2}$	−4.806	−5.430	−6.136	−3.456	−3.517		
Second derivative	$a_0\sqrt{3}/2$	18.13	21.41	27.35	7.67	1.54		
	a_0	19.75	23.77	30.38	8.86	4.78		
$\frac{R^2}{f}\frac{d^2f}{dR^2}$	$a_0\sqrt{2}$	25.57	31.90	40.73	13.88	12.70		

[a] Crystal-field splitting between the $4d$ and the $5s$ orbitals.
[b] Crystal-field splitting between the e ($d_{z^2}, d_{x^2-y^2}$) and the t (d_{xy}, d_{xz}, d_{yz}) orbitals.
[c] $a_0=6.2294$ a.u..

$$C' = G_1 = \tfrac{1}{2}(C_{11} - C_{12}) \tag{10b}$$

is the tetragonal mode shear constant, and

$$G_2 = C_{44} \tag{10c}$$

is the trigonal-mode shear constant.

Tetragonal and trigonal shears are double and triply degenerate, respectively. To simplify the calculations we choose special symmetric deformations of those types. We make the calculation for the following three strains:

(i) *Homogenous expansion.*

$$\epsilon_1 = \epsilon_2 = \epsilon_3 = \gamma_0\,, \qquad \epsilon_4 = \epsilon_5 = \epsilon_6 = 0\,. \tag{11a}$$

(ii) [001] *symmetric tetragonal shear.*

$$-2\epsilon_1 = -2\epsilon_2 = \epsilon_3 = \gamma_1\,, \qquad \epsilon_4 = \epsilon_5 = \epsilon_6 = 0\,. \tag{11b}$$

(iii) [111] *symmetric trigonal shear.*

$$\epsilon_1 = \epsilon_2 = \epsilon_3 = 0\,, \qquad \epsilon_4 = \epsilon_5 = \epsilon_6 = \gamma_2\,. \tag{11c}$$

For each of these deformation the bilinear increase in the free energy per unit volume is given by

$$\delta F(\gamma_\lambda) = \tfrac{3}{2} G_\lambda \gamma_\lambda^2 \quad (\lambda = 0, 1, 2)\,. \tag{12}$$

So the elastic constants can be calculated differentiating the free energy with respect to the appropriate strain:

$$G_\lambda = \tfrac{1}{3}\left(\frac{\partial^2 F}{\partial \gamma_\lambda^{\,2}}\right)_0 \tag{13}$$

Using a noninteracting-particle type of free energy one obtains the following expressions for G_λ:

$$G_\lambda = \tfrac{2}{3}\sum_{b\vec{k}}\left[f(E_{b\vec{k}})\left(\frac{\partial^2 E_{b\vec{k}}}{\partial \gamma_\lambda^{\,2}}\right)_0 + \left(\frac{\partial f(E_{b\vec{k}})}{\partial \gamma_\lambda}\right)_0\left(\frac{\partial E_{b\vec{k}}}{\partial \gamma_\lambda}\right)_0\right], \tag{14}$$

where f is the Fermi function.

The strain derivatives of the Fermi function are given by

$$\frac{\partial f(E_{b\vec{k}})}{\partial \gamma_\lambda} = \frac{df(E_{b\vec{k}})}{dE_{b\vec{k}}}\left(\frac{\partial E_{b\vec{k}}}{\partial \gamma_\lambda} - \frac{\partial E_F}{\partial \gamma_\lambda}\right) \tag{15}$$

and the Fermi energy derivatives are obtained from the number of particles conservation:

$$\frac{\partial E_F}{\partial \gamma_\lambda} = \left(\sum_{\vec{k}} \frac{df(E_{b\vec{k}})}{dE_{b\vec{k}}}\,\frac{\partial E_{b\vec{k}}}{\partial \gamma_\lambda}\right) \Big/ \left(\sum_{b\vec{k}} \frac{df(E_{b\vec{k}})}{dE_{b\vec{k}}}\right). \tag{16}$$

This derivative vanishes for $\lambda = 1, 2$ as was shown in Ref. 16.

In order to obtain the strain derivatives of the band energies we expand the electrons single-particle Hamiltonian matrix in power series of the strain γ_λ:

$$\underline{H}(\vec{k}, \gamma_\lambda) = \sum_{n=0}^{\infty} \frac{1}{n!}\,\gamma_\lambda^n \underline{H}^{(\lambda, n)}(\vec{k})\,. \tag{17}$$

Working in the undistorted lattice-band representation, in which $H_{bb'}^{(\lambda,0)}(\vec{k}) = \delta_{bb'} E_{b\vec{k}}$, we can apply a perturbation expansion and get

$$\left(\frac{\partial E_{b\vec{k}}}{\partial \gamma_\lambda}\right)_0 = H_{bb}^{(\lambda,1)}(\vec{k})\,, \tag{18a}$$

$$\left(\frac{\partial^2 E_{b\vec{k}}}{\partial \gamma_\lambda^{\,2}}\right)_0 = H_{bb}^{(\lambda,2)}(\vec{k}) + 2\sum_{b'}{}' \frac{|H_{bb'}^{(\lambda,1)}(\vec{k})|^2}{E_{b\vec{k}} - E_{b'\vec{k}}}\,. \tag{18b}$$

Inserting (15) and (18) in Eq. (14) we get the following expression for the elastic constants:

$$G_\lambda = \tfrac{2}{3}\sum_{b\vec{k}} H_{bb}^{(\lambda,2)}(\vec{k}) f(E_{b\vec{k}}) + \sum_{bb'\vec{k}} H_{bb'}^{(\lambda,1)}(\vec{k}) * \times\left(H_{b'b}^{(\lambda,1)}(\vec{k}) - \delta_{bb'}\frac{\partial E_F}{\partial \gamma_\lambda}\right) \times \frac{f(E_{b\vec{k}}) - f(E_{b'\vec{k}})}{E_{b\vec{k}} - E_{b'\vec{k}}}\Bigg], \tag{19}$$

where the second sum is taken also for $b = b'$ obtaining $df(E)/dE$ as a limit.

Equation (19) could be also obtained by a diagramatic approach calculating the electronic contribution to the zero-momentum-limit acoustic phonons. The elastic constants G_λ are proportional to $\lim_{q\to 0}[\Omega_\lambda(\vec{q})/q]^2$, $\Omega_\lambda(\vec{q})$ being the appropriate phonon frequency [see Eq. (1)]. The matrix elements $H_{bb'}^{(\lambda,n)}(\vec{k})$ are proportional to $\lim_{q\to 0}[g_{bb'}^{(\lambda,n)}(\vec{k},\vec{q})/q^n]$, $\underline{g}^{(\lambda,n)}(\vec{k},\vec{q})$ being the appropriate nth-order electron-phonon coupling matrix based on wave functions which follow the atomic displacements. In Ref. 18, the same method and band parameters used here are applied to calculate the first order electron-phonon coupling matrix elements, solving the superconducting Eliashberg equations.

In our tight-binding scheme, the $\underline{H}^{(\lambda,n)}(\vec{k})$ matrices are related to strain derivatives of the space Hamiltonian matrix $\underline{H}(\vec{R})$ by [see Eq. (6)]

$$\underline{H}^{(\lambda,n)}(\vec{k}) = \sum_{\vec{R}} e^{i\vec{k}\cdot\vec{R}}\,\underline{U}(\vec{k})^\dagger \underline{H}^{(\lambda,n)}(\vec{R})\underline{U}(\vec{k})\,. \tag{20}$$

In order to calculate the derivatives $\underline{H}^{(\lambda,n)}(\vec{R})$, $n = 1, 2$, we need the first and second R (distance) derivatives of the band parameters given in Table II; we need the first and second l_i (direction cosines) derivatives of the angular coefficients used to construct $\underline{H}(\vec{R})$, given from expressions in Refs. 16 and 26; and finally we need the first and second strain (γ_λ) derivatives of R and l_i. The first strain derivatives $\partial R/\partial\gamma_\lambda$ and $\partial l_i/\partial\gamma_\lambda$ are obtained using Eqs. (7), (8), (11), and given in

TABLE III. Strain derivatives of the distance R and of the directions cosines l_i $(i=1,2,3)$ for the strains γ_λ $(\lambda=0,1,2)$ defined in the text.

Strain	$\frac{\partial R}{\partial \gamma_\lambda}$	$\frac{\partial l_i}{\partial \gamma_\lambda}$
Expansion $\lambda=0$	R	0
Tetragonal $\lambda=1$	$\frac{1}{2}R(3l_3^2-1)$	$-\frac{3}{2}l_i l_3^2$, $i=1,2$ $\frac{3}{2}l_3(1-l_3^2)$, $i=3$
Trigonal $\lambda=2$	$\frac{1}{2}R\sum_{j,k\neq j} l_j l_k$	$\frac{1}{2}\sum_{j\neq i} l_j - \frac{1}{2}l_i\sum_{j,k\neq j} l_j l_k$

Table III. A finite strain γ_λ is constructed as an integral of infinitesimal strains $d\gamma_\lambda$, each of them defined by Eqs. (7), (8), and (11) (replacing these $\bar{\epsilon}$, ϵ and γ by $d\bar{\epsilon}$, $d\epsilon$, and $d\bar{\gamma}$). So the second strain derivatives $\partial^2 R/\partial\gamma_\lambda^2$ and $\partial^2 R/\partial\gamma_\lambda^2$ are obtained by differentiating the first derivatives expressions given in Table III, using those expressions again for the required derivatives of R and l_i.

The $\underline{H}^{(\lambda,n)}(\vec{k})$ matrices are not invariant under the cubic star transformations group, but under its subgroup, the star transformation of the γ_λ deformed lattice. However, for any cubic star operation s, there exists a unitary matrix $\underline{T}(s)$, which can be obtained simply from symmetry considerations, and which yields for any $\vec{k}$

$$\underline{U}(s\vec{k}) = \underline{T}(s)\underline{U}(\vec{k}) . \tag{21}$$

So actually one has to do the diagonalization procedure (6) only for points $\vec{k}$ in the cubic irreducible Brillouin zone (IBZ), and to evaluate once and for all the matrices

$$\underline{H}^{(n)}(\vec{R}, s_\lambda) = \underline{T}(s_\lambda)^\dagger \underline{H}^{(\lambda,n)}(\vec{R})\underline{T}(s_\lambda) , \tag{22}$$

where s_λ are the star operations generating the γ_λ deformed IBZ out of the cubic one (there are 1, 3, and 4 such operations for $\lambda=0$, 1, and 2, respectively).

The required expression for $\underline{H}^{(\lambda,n)}(\vec{k})$ in a $\vec{k}$ point of the deformed lattice IBZ, in terms of the eigenvectors matrix in a $\vec{k}$ point of the cubic IBZ, is obtained inserting (21) and (22) in (20) and given by

$$\underline{H}^{(\lambda,n)}(s_\lambda k) = \sum_{\vec{R}} e^{i(s_\lambda\vec{k})\cdot\vec{R}} \underline{U}(\vec{k})^\dagger \underline{H}^{(n)}(\vec{R}, s_\lambda)\underline{U}(\vec{k}) . \tag{23}$$

C. Computational procedure

The elastic constants are computed on the basis of Eq. (19) (and the equations related to it), taking 1015 points in the cubic IBZ. Convergence in the whole temperature range is obtained using a new interpolation method[27] which enables making second-order energy interpolation with rather simple expressions.

The distance-dependent parametrization makes it possible to calculate the effect of volume change due to temperature and alloying on the band structure. For this purpose we use tabulated temperature-dependent thermal-expansion coefficients of Nb,[28] and the previously measured[14] lattice constants for the Nb-Zr alloys. As for the thermal expansion coefficients in the alloys, their deviation from the pure Nb values has been measured and found not to exceed several percent, which permits using the Nb coefficient instead without a considerable effect on the results. Alloying effects not connected with the volume change are neglected within our approximation.

There are two types of temperature effects, the first due to the Fermi function in Eq. (19) and the second due to thermal expansion. The second effect is found to be a linear decrease in the absolute values of the elastic constants with temperature, at a rate closely proportional to their magnitudes. Such an expansion anharmonic effect is the major reason for the normal linear decrease of elastic constants with temperature.[29]

Following the procedure explained in the Sec. II we get for pure Nb at zero temperature $C_{44}=-3.55$, $C'=0.19$, and $B=-2.13$ in units of 10^{11} N/m^2. The negative values reflect well what in classical works[30] is called "Fermi contributions" which are attractive.

In the present calculation there have been several inaccuracies and terms which are not included: (i) neglect of contributions from inner-shell electrons and nuclei and this is just the so called "repulsive part" in the elastic constants[31]; (ii) double counting of electron-electron interaction contribution to the band energies in Eq. (14) due to the use of a noninteracting-particle free energy; (iii) neglect of the distance dependence of crystal-field integrals; (iv) inaccuracies due to parametrization and the band structure used here; and (v) neglect of alloying effects other than volume changes.

The missing terms and inaccuracies are believed to have no essential effect on the anomalous behaviour of the elastic constants. However, those terms naturally decrease with volume similarly to the included terms. The missing terms are accounted by adding "calibration" factors to each of the elastic constants which match the pure-Nb zero-temperature results to the experimental ones. Those calibration factors have to be volume dependent to account for the variation of the missing terms with volume. As a first approximation we take the volume dependence of the calibration terms to be proportional to the volume dependence

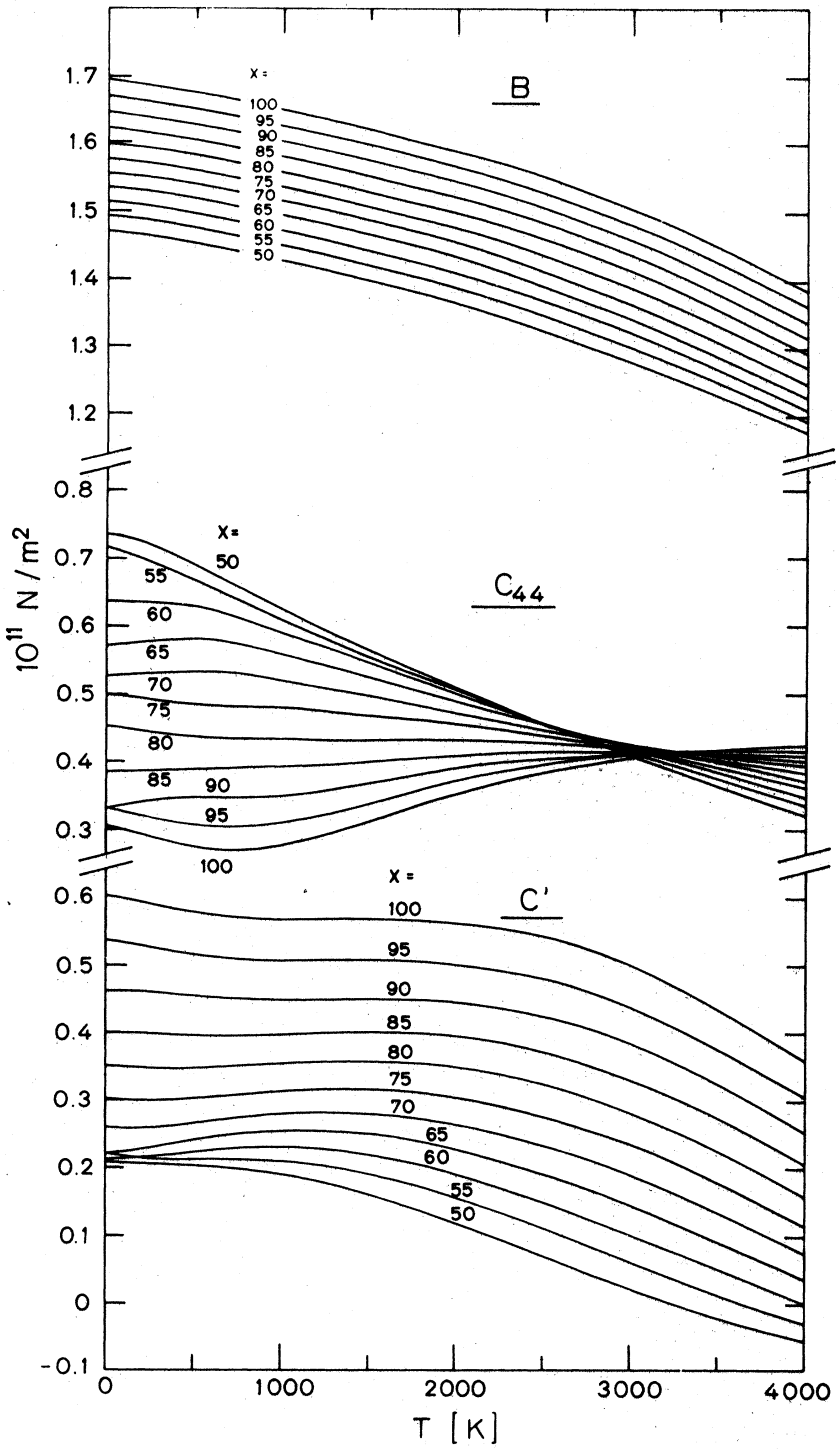

FIG. 6. Theoretical results for the elastic constants in Nb_xZr_{100-x}.

of the included terms of each elastic constant for zero-temperature pure Nb. The same calibration term modified by the volume changes is added to all the curves of the same elastic constant.

The calculation is done over a wide temperature range, with the Nb content in the alloy varied between 100 and 50 at.%. The results obtained for C_{44}, C', and B are shown in Fig. 6.

IV. DISCUSSION

There is an agreement between the theoretical and the experimental results (Figs. 3, 5, and 6)

regarding the variation of the elastic constants with alloying and temperature, the shift of the low-temperature minimum in C_{44}, the crossing of the C_{44} curves, and the decrease of the slopes at high temperatures.

As was discussed in Sec. II the effect of the volume with temperature introduces an approximatively linear negative slope to the theoretical results.

Doing a constant-volume calculation, a positive slope increment has to be added in agreement with constant-volume experimental results for pure Nb in the 300–450-K range derived from measurements under pressure (H. Lê Huy, C. Weinmann, and S. Steinemann, private communication). From this work it seems that the main origin of the normal linear decrease of elastic constants with temperature is due to the volume increase and not to the other types of anharmonic effects.[29]

The anomalous behaviour of C_{44} is a Fermi-surface (FS) effect due to the first derivative term in Eq. (19). It originates from the high-density-of-states region situated in the Brillouin zone between the jungle-gym and the ellipsoid FS sheets (Fig. 1) and disturbed mainly by a C_{44} type of deformation. The C_{44} anomaly at low temperatures is also expressed through its increase with the Zr content in contrast to C' and B. As temperature becomes higher, the C_{44} curves cross, and then they decrease with the Zr content like the other elastic constants.

The decrease in the slopes of the elastic constant at high temperatures seems to be associated with the fact that a considerable number of electrons start to be excited from another branch in the dispersion curves around the point P (Fig. 1). As Zr is alloyed, the Fermi level goes down, and the temperature at which electrons start to be excited from this region goes down too, giving the right experimental effect of alloying on the slope decrease temperature. As suggested in a previous work[15] a second-order anharmonic effect can also contribute to such a decrease.

A problem associated with this work is whether the rigid-band approximation for the alloys is valid. Otherwise, one should use such methods as Miedma's approach[32] of the CPA (coherent-potential approximation), or make a supercell calculation. From this work and from recent work by Katahara *et al.*,[33] it seems that the rigid-band approximation works over a wide range of compositions for alloys of transition metals of the fifth column with ones of the fourth or the sixth column and the same row. On the other hand, in measurements done on Pd-Rh and Pd-Ag alloys,[34] a similar shift of a minimum in C_{44} was observed for a few percent of the alloyed metal. For a higher percentage, the structure in C_{44} disappears which might indicate the breakdown of the rigid-band approximation in that substance.

Another problem is whether the present calculation treats correctly the charge rearrangement due to the deformation. Sinha and Harmon[8] and Hanke *et al.*[35] have calculated phonon anomalies resulting from charge fluctuations, and have shown that the anomalous magnitude has a direct relation to the density of states. In our work charge rearrangement is probably accounted well in the tight-binding limit.[17] However, an additional screening calculation of that type[8,35] could probably improve the agreement of C_{44} with experiment, especially the correlation of the zero-temperature results with the density of states at the Fermi level of the alloy.

V. CONCLUSION

The elastic constants of bcc Nb-Zr alloys have been investigated intensively both by experiment and theory. Results have been obtained for Nb with 0 to 70-at.% Zr and temperatures between zero and the melting point, making ultrasonic measurements on single crystals using a long Nb wave guide for high temperature.

A first-principles calculation explains qualitatively the anomalous behavior obtained experimentally, and also the normal decrease effect. The calculation is based on the band structure in the vicinity of the Fermi level, and on a tight-binding parametrization scheme used to derive the electron lattice coupling constants. It is of a type similar to phonon dispersion calculations,[9] having a further difficulty of convergence in the whole temperature range which is overcome using a second-order interpolation method.[27]

In order to obtain a better quantitative agreement between theory and experiment, one has first of all to improve the band parametrization scheme, and the linear muffin-tin orbital (LMTO) method of Andersen[36] seems to be useful. Using the virial theorem as done by Pettifor[37] might help solving the double counting problem. The core electrons and nuclei have to be considered, and more care has to be taken for deformation charge rearrangement[8,35] and alloying[32] problems. Finally, the contribution of the phonons to the elastic constants and their temperature dependence will have to be more fully discussed in the future.[38]

ACKNOWLEDGMENT

The authors acknowledge the technical help of C. Chevalier, the valuable assistance of P. A. Maeusli, and stimulating discussions with D. Bichsel.

[1]L. F. Mattheiss, Phys. Rev. B 1, 373 (1970).
[2]N. Elyashar and D. D. Koelling, Phys. Rev. B 15, 3620 (1977).
[3]O. K. Andersen, Phys. Rev. B 2, 883 (1970).
[4]F. M. Mueller, A. J. Freeman, J. O. Dimmock, and A. M. Furdyna, Phys. Rev. B 1, 4617 (1970).
[5]F. Y. Fradin, D. D. Koelling, A. J. Freeman, and T. J. Watson-Yang, Phys. Rev. B 12, 5570 (1975).
[6]Y. Nagakawa and A. D. B. Woods, in *Lattice Dynamics*, edited by R. F. Wallis (Pergamon, New York, 1963).
[7]R. I. Sharp, J. Phys. C 2, 421 (1969); 2, 432 (1969).
[8]S. K. Sinha and B. N. Harmon, in *Superconductivity in d- and f-Band Metals*, edited by D. H. Douglass (Plenum, New York, 1976), p. 269; B. N. Harmon and S. K. Sinha, *ibid.* p. 391.
[9]C. M. Varma and W. Weber, Phys. Rev. Lett. 39, 1094 (1977); C. M. Varma, P. Vashishta, E. I. Blount, and W. Weber (unpublished).
[10]J. K. Hulm and R. D. Blaugher, Phys. Rev. 123, 1569 (1961).
[11]P. E. Armstrong, J. M. Dickinson, and M. L. Brown, Trans. Met. Soc. AIME 236, 1404 (1966).
[12]D. J. Hayes and F. R. Brotzen, J. Appl. Phys. 45, 1721 (1974).
[13]C. Goasdoue, P. S. Ho, and C. L. Sass, Acta Metall. 20, 725 (1976).
[14]E. Walker and M. Peter, J. Appl. Phys. 48, 2820 (1977).
[15]Y. Talmor, E. Walker, and S. Steinemann, Solid State Commun. 23, 649, (1977).
[16]M. Peter, W. Klose, G. Adam, P. Entel, and E. Kudla, Helv. Phys. Acta 47, 807 (1974).
[17]J. Ashkenazi, M. Dacorogna, and M. Peter (unpublished).
[18]M. Peter, J. Ashkenazi, and M. Dacorogna, Helv. Phys. Acta 50, 267 (1977).
[19]D. P. Karim, J. B. Ketterson, and G. W. Crabtree, J. Low Temp. Phys. 30, 389 (1978).
[20]J. Ashkenazi, M. Dacorogna, M. Peter, Y. Talmor, and E. Walker, in *Transition Metals 1977*, (Conference Series No. 39) edited by M. J. G. Lee, J. M. Perz, and E. Fawcett (The Institute of Physics, Bristol and London, 1978), p. 695.
[21]R. Lowrie and A. M. Gonas, J. Appl. Phys. 36, 2189 (1965).
[22]J. Ashkenazi and M. Weger, J. Phys. Chem. Solids 33, 631 (1972).
[23]M. Weger and I. B. Goldberg, in *Solid State Physics*, edited by H. Ehrenreich, F. Seitz, and D. Turnbull, (Academic, New York, 1973) Vol. 28, p. 1.
[24]A. Birnboim and H. Gutfreund, Phys. Rev. B 12, 2682 (1975).
[25]D. G. Pettifor, J. Phys. C 2, 1051 (1969); 5, 97 (1972).
[26]M. Peter and G. Adam, Rev. Roum. Phys. 21, 385 (1976).
[27]J. Ashkenazi and M. Peter (unpublished).
[28]*American Handbook of Physics* (McGraw-Hill, New York, 1963), pp. 4–67.
[29]G. Leibfried and W. Ludwig, in Solid State Physics, edited by F. Seitz and D. Turnbull, (Academic, New York), Vol. 12, p. 276; W. Ludwig, *Springer Tracts in Modern Physics* (Springer Verlag, Berlin, Heidelberg, New York, 1967), p. 431.
[30]K. Fuchs, Proc. R. Soc. A 153, 622 (1936); 157, 444 (1936); R. S. Leigh, Philos, Mag. 42, 139 (1951).
[31]F. Ducastelle, J. Phys. (Paris) 31, 1055 (1970).
[32]A. R. Miedema, J. Phys. F 3, 1803 (1973); 4, 120 (1974).
[33]K. W. Katahara, N. H. Manghnani, and E. S. Fisher, in Ref. 20, p. 414.
[34]E. Walker, J. Ortelli, and M. Peter, Phys. Lett. A 31, 240 (1970).
[35]W. Hanke, J. Hafner, and H. Bilz, Phys. Rev. Lett. 37, 1560 (1976).
[36]O. K. Andersen, Phys. Rev. B 12, 3060 (1975).
[37]D. G. Pettifor, Commun. Phys. 1, 141 (1976).
[38]D. Bichrel (private communication).